

## Improving the Mechanical Properties of Polyamide 6-Nanosilica Nanocomposites by Combining Masterbatch Technique with *in situ* Polymerization

Qijie Xu,<sup>\*,a,b</sup> Xiaohong Li,<sup>a</sup> Fangfei Chen<sup>a</sup> and Zhijun Zhang<sup>a</sup>

<sup>a</sup>Key Laboratory of Ministry of Education for Special functional Materials, Henan University, Kaifeng 475004 Henan, China

<sup>a</sup>Department of Chemistry & Chemical Engineering, Huanghuai University, Zhumadian 463000 Henan, China

Um *masterbatch* (MA) reativo de poliamida 6 (PA6)/SiO<sub>2</sub> contendo 20% (fração de massa) de nano-SiO<sub>2</sub> foi preparado. Posteriormente, o MA reativo preparado foi usado como carga no preparo de nanocompósitos PA6/SiO<sub>2</sub> (RA). A estrutura do RA foi analisada por espectrometria no infravermelho por transformada de Fourier (FTIR), microscopia eletrônica de transmissão (TEM), difratometria de raios X (XRD), microscopia eletrônica de varredura (SEM) e microscopia óptica de luz polarizada (POM). A estabilidade térmica e o comportamento de cristalização do RA foram avaliados por análise termogravimétrica (TGA) e calorimetria exploratória diferencial (DSC). OS resultados indicaram que as cadeias moleculares de PA6 estavam ancoradas na superfície do nano-SiO<sub>2</sub> através de ligações químicas entre a superfície de grupos amino do nano-SiO<sub>2</sub> e do monômero da  $\epsilon$ -caprolactama ou pré-polímero da PA6. Como resultado, uma camada interfacial flexível foi formada, melhorando a compatibilidade do nano-SiO<sub>2</sub> com a matriz de PA6. Além disso, o efeito no nano-SiO<sub>2</sub> apresentou melhoras nas propriedades mecânicas do RA. Devido ao efeito de impedimento de movimento das cadeias moleculares da PA6 pelas partículas de nano-SiO<sub>2</sub>, o tamanho da esfera cristalina de PA6 foi menor e sua forma cristalina também foi afetada. A massa molar da matriz de PA6 tende a decair gradualmente com o aumento do conteúdo nano-SiO<sub>2</sub>.

A reactive polyamide 6 (PA6)/SiO<sub>2</sub> masterbatch (MA) containing 20% (mass fraction) of nano-SiO<sub>2</sub> was prepared readily. Furthermore, the as-prepared reactive MA was used as a filler to prepare PA6/SiO<sub>2</sub> nanocomposites (RA). The structure of RA was analyzed by means of Fourier transform infrared spectrophotometry (FTIR), transmission electron microscopy (TEM), powder X-ray diffractometry (XRD), scanning electronic microscopy (SEM) and polarizing microscopy (POM). Thermal stability and crystallization behaviors of RA were evaluated by thermogravimetric analysis (TGA) and differential scanning calorimetry (DSC). Findings indicated that the PA6 molecular chains were anchored on the surface of nano-SiO<sub>2</sub> through chemical bonding between the surface amino groups of nano-SiO<sub>2</sub> and  $\epsilon$ -caprolactam monomer or prepolymer of PA6. As a result, a flexible interfacial layer was formed, thereby improving the compatibility of nano-SiO<sub>2</sub> with PA6 matrix. Moreover, the enhancement effect of nano-SiO<sub>2</sub> led to the improved mechanical properties of RA. Besides, due to the hindering effect of nano-SiO<sub>2</sub> particles to the movement of PA6 molecular chains, the size of the PA6 spherocrystal was smaller, and its crystalline form was also affected. Furthermore, the molecular weight of the PA6 matrix tended to decrease gradually with increasing nano-SiO<sub>2</sub> content.

**Keywords:** PA6, nano-SiO<sub>2</sub>, masterbatch technique, *in situ* polymerization, composites

### Introduction

Polymer-matrix composites (PMCs) continually grasp human's interest for decades, because they possess markedly improved mechanical properties (tensile modulus

and strength), thermal stability, chemical resistance, flame retardancy, and barrier resistance as compared with pure polymers.<sup>1-3</sup> Usually, the improved properties of PMCs are highly dependent on the nature of filler, the interfacial interaction between filler and polymeric matrix, and the compatibility and dispersibility of the filler.<sup>4,5</sup> As to conventional composites, the enhancement in the desired

\*e-mail: qijie01@tom.com

properties is often accompanied by trade-offs in other properties.<sup>6,7</sup> For example, the improvement of tensile strength of polymeric materials is commonly accompanied by reduced ductility and toughness.<sup>8-10</sup> Differing from conventional composites, nanocomposites often exhibit properties that are dramatically different from those of micrometer scale counterparts while no significant trade-offs of mechanical properties emerge. This means that multifunctionalized PMCs with significantly improved mechanical properties could be developed by miniaturizing the size of fillers to nanoscale level. Unfortunately, the commonly used molten mixing method for preparing polymer-matrix nanocomposites faces drawbacks in that inorganic nanoparticles (i.e., fillers) are highly reactive and liable to dust pollution and agglomeration. To get rid of these drawbacks, researchers have tried to improve the dispersion of nanoscale fillers in polymer matrices and increase the interfacial interaction between the filler and the polymer matrix by making use of sizing agents, surface-modifying agents and other promoters.<sup>11,12</sup> Such strategies, however, are often limited by low efficiency and poor feasibility for industrialization.

To overcome the disadvantages of the above-mentioned strategies, we specially focus on preparing polymer-matrix nanocomposites by combining the masterbatch method with *in situ* polymerization route. Namely, the desired masterbatch with a high content of silica nanoparticles is prepared by the molten mixing technique and the as-obtained masterbatch is then diluted with polymer matrix to prepare nanocomposites via *in situ* polymerization.<sup>9,13-15</sup> In such a way, the dispersion of inorganic nanoparticles in the polymer matrix can be greatly improved, and the process for preparing PMCs is effectively simplified. Conventional masterbatches (though possessing good dispersibility in polymeric matrix), nevertheless, are unable to continually react with polymeric materials affording PMCs possessing strong interfacial bonding, due to lack of interfacial chemical bonding. Therefore, in this research we developed a reactive polymerized  $\epsilon$ -caprolactam masterbatch containing a high content of surface-capped nano-SiO<sub>2</sub>, in which the nano-SiO<sub>2</sub> particles were modified *in situ* by silane coupling agent 3-triethoxysilylpropylamine containing amino functional groups. The as-obtained reactive masterbatch was then used as a filler to fabricate polyamide 6 (PA6)/nano-SiO<sub>2</sub> nanocomposites by *in situ* polymerization. Thanks to the incorporation of the reactive amino functional group, the as-obtained masterbatch containing nano-SiO<sub>2</sub> can be well dispersed in the PA6 matrix and possesses improved compatibility with the polymer matrix. Furthermore, the formation of local "micro-network" structure (as seen in Figure 1) and flexible interface on nano-SiO<sub>2</sub> surface also favors to enhance the mechanical strength of

nanocomposites. Such a strategy, hopefully, may be utilized to afford novel multifunctionalized PA6 nanocomposite with greatly improved mechanical properties.

## Experimental

### Materials

Nano-SiO<sub>2</sub> surface-modified by 3-triethoxysilylpropylamine, a silane coupling agent, was obtained from Henan Research Center of Nanomaterials Engineering & Technology (Jiyuan, China). Reagent grade  $\epsilon$ -caprolactam was kindly provided by Yelang Chemical Company Limited (Wuhan, China). Reagent grade adipic acid was supplied by Painsi Chemical Reagent Factory (Zhengzhou, China). Reagent grade formic acid was supplied by Kemel Chemical Reagent Company Limited (Tianjin, China).

### Preparation of masterbatch and PA6/nano-SiO<sub>2</sub> nanocomposites

100.0g of  $\epsilon$ -caprolactam, 1.0 g of adipic acid (used as blocking agent and catalyst), 25 g of nano-SiO<sub>2</sub> and 2.0 mL of distilled water were added to a 250 mL three-neck flask. Resultant mixture was heated from room temperature to 190 °C with an electric heating jacket under stirring and allowed to react for about 3 h thereat. Then the reaction system was gradually heated to 260 °C within 1.5-2.0 h, followed by gradual pumping to -0.08 MPa within about 1.5 h affording crude masterbatch containing 20% nano-SiO<sub>2</sub>.

PA6/SiO<sub>2</sub> nanocomposites (RA) were prepared in similar manners. Briefly, different amounts of masterbatch (0.5 g, 1.5 g, 2.5 g, 3.5 g and 4.5 g, respectively, that was, the actual nano-SiO<sub>2</sub> content was 0.1 g, 0.3 g, 0.5 g, 0.7 g and 0.9 g), 1.0 g of adipic acid, 100 g of  $\epsilon$ -caprolactam, and 2.0 g of distilled water were added to a 250 mL three-neck flask and allowed to react under the aforementioned conditions to afford crude nanocomposites. The above steps of the synthesis are illustrated in Figure 1. And then, as-obtained crude nanocomposites were cast molded into dumbbell-like and spline-like specimens for evaluation of mechanical properties. Cast molded nanocomposite specimens were dried at 80 °C in an oven for 24 h and then used for characterization of structure and evaluation of mechanical properties.

### Extraction of nano-SiO<sub>2</sub> from masterbatch and PA6/nano-SiO<sub>2</sub> nanocomposites

Proper amounts of as-obtained masterbatch and cast molded RA were separately dissolved in formic acid and

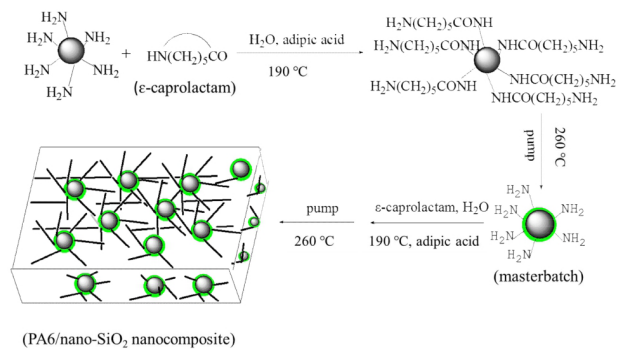


**Figure 1.** Schematic diagram showing stepwise synthesis of RA.

repeatedly dispersed/centrifuged for 6 cycles so as to extract nano-SiO<sub>2</sub> (as-extracted nano-SiO<sub>2</sub> were denoted as CMA and CRA, respectively). Upon completion of the last cycle of dispersion/centrifuging, PA6 could not be detected in suspension by infrared spectrometry (IR).<sup>16</sup>

Characterization of structure and evaluation of mechanical properties

Fourier transform infrared spectrophotometry (FTIR) spectra were recorded with an Avatar360 Fourier transform infrared spectrophotometer (FTIR, Nicolet, USA; KBr pellet). Thermogravimetric analysis (TGA) and differential thermogravimetric (DTG) analysis of as-fabricated RA were conducted with a TG/SDTA851<sup>o</sup> system (Mettler Toledo, Switzerland; up to 1000 °C, heating rate 10 °C min<sup>-1</sup>). A transmission electron microscopy (TEM, Amsterdam, Netherlands) was performed at an accelerating voltage of 30 kV to observe the state of nano-SiO<sub>2</sub> in PA6 matrix, with which nano-SiO<sub>2</sub> was extracted from RA containing 0.5% nano-SiO<sub>2</sub> content by dissolving in formic acid. A scanning electronic microscopy (SEM, JSM 5600LV, Japanese electronics, Japan) was used for examining the impact fracture surface of PA6 and RA at an accelerating voltage of 30 kV, with which the fracture surface of specimens were sputter-coated with gold prior to observation. X-ray diffraction patterns (XRD, Philips, Holland) were recorded with a D/max 2550 V X-ray diffractometer (Cu K $\alpha$  radiation,  $\lambda = 1.54178 \text{ \AA}$ ) to examine the crystalline forms of samples, with which the samples were dried in an oven at 80 °C for 24 h. The diffractometer patterns were collected from 5-30° with a step interval of 0.04°. The morphology of spherulite PA6 and its nanocomposites was observed with a Leica DMLP polarizing optical microscopy equipped with a Linkam TM600 hot stage. The crystallization and melting behaviors of PA6 and RA were investigated by differential scanning calorimetry [DSC; DSC822<sup>o</sup>, Mettler-Toledo, Switzerland; about 5 mg of to-be-tested samples was heated from room

temperature (20 °C) to 300 °C at a rate of 10 °C min<sup>-1</sup> and then cooled down to room temperature].

The tensile strength of PA6 and RA were measured with a WDW-10D testing machine according to Chinese National standard GB/T 1040-1992. The impact strength was evaluated with a ZBC-1400-2 testing machine according to Chinese National standard GB/T 1040-1993. Besides, a ubbelohde viscometer was used to determine the viscosity average molecular weight of PA6 in RA, and the specimens to be tested were obtained after as-prepared RA were repeatedly dissolved in formic acid and centrifuged for 3 times.

## Results and Discussion

FTIR analyses of PA6, nano-SiO<sub>2</sub>, CRA and CMA

FTIR spectra are measured to verify whether nano-SiO<sub>2</sub> is chemically bonded with PA6 molecular chains. That is because that the chemical bonding can result in greatly improved compatibility of nano-SiO<sub>2</sub> with PA6 matrix, moreover, significantly increased interfacial strength between the inorganic filler and the polymer matrix. Figure 2 shows the FTIR spectra of PA6, nano-SiO<sub>2</sub>, CRA, and CMA. CRA and CMA are obtained via repeated dispersion/centrifugation until PA6 could not be detected in suspension by IR. Therefore, we can infer that any homopolymers based on physical absorption should not remain on the surface of as-measured CRA and CMA. The absorption peaks of CRA and CMA at 1646 cm<sup>-1</sup> and 1558 cm<sup>-1</sup> are assigned to polyamide, the one at 3431 cm<sup>-1</sup> corresponds to N-H bond, and those at 2950 cm<sup>-1</sup> and 2875 cm<sup>-1</sup> are assigned to C-H bond. These observations reveal that CRA and CMA are coated with the molecular chains of PA6, which demonstrates that it is feasible to establish a chemical bonding between nanoparticulates (nano-SiO<sub>2</sub>) and polymer matrix (PA6) by making use

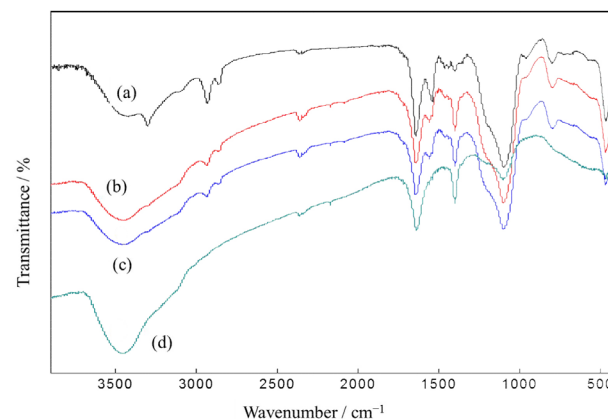


**Figure 2.** FTIR spectra of PA6 (a), nano-SiO<sub>2</sub> (d), CRA (b) and CMA (c).

of functionalized nano-SiO<sub>2</sub>.<sup>16-18</sup> It is just the chemically bonded interfacial layer that functions to greatly improve the dispersion of nano-SiO<sub>2</sub> in PA6 matrix and enhance its compatibility with the polymer matrix, thereby increasing the interfacial strength between nano-SiO<sub>2</sub> and PA6 matrix.

#### TG and DTG analyses of PA6, nano-SiO<sub>2</sub>, CRA and CMA

The content of PA6 on nano-SiO<sub>2</sub> surface also greatly affects the compatibility and interfacial strength of nano-SiO<sub>2</sub> with PA6. Figure 3 shows the TG and DTG curves of PA6, nano-SiO<sub>2</sub>, CMA, and CRA. The weight loss of nano-SiO<sub>2</sub> is less than that of CRA and CMA, and the weight loss of CRA is obviously higher than that of CMA. This indicates that CRA extracted from as-fabricated RA has a higher content of grafted PA6 than CMA extracted from as-obtained masterbatch. Particularly, the weight loss of CRA is higher than that of PA6-matrix composites prepared by other methods, such as molten mixing method and only *in situ* polymerization method.<sup>12,19</sup> It illustrates that the surface of nano-SiO<sub>2</sub> can form more strong interfacial strength by using the method of this paper that is beneficial to improve the mechanical properties of PA6. The possible reasons are as follow. During the preparation of masterbatch, the grafted-PA6 molecular chains on the surface of nano-SiO<sub>2</sub> are very hard to form longer molecular chains. That is because that the plenty of amino activated points of nano-SiO<sub>2</sub> can participate in the polymerization process of monomer, thereby containing much amino groups in masterbatch. However, the amino group of reactive masterbatch as fillers can continually react with monomer or prepolymer to participate in the preparation process of RA and allows formation of longer PA6 molecular chains.<sup>20,21</sup> As a result, CRA extracted from as-fabricated RA has a larger weight loss than CMA, nano-SiO<sub>2</sub>.

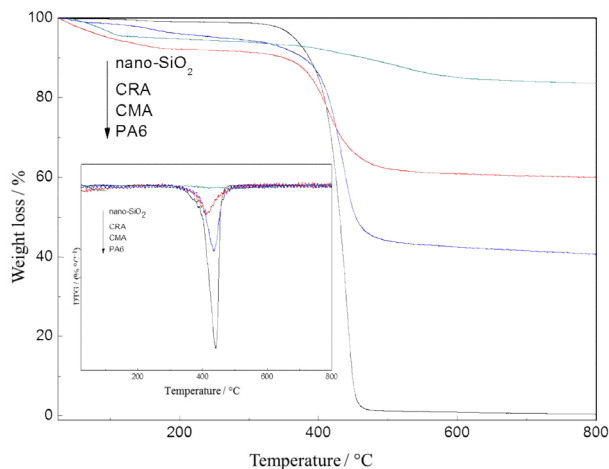


**Figure 3.** TG and DTG curves of PA6, nano-SiO<sub>2</sub>, CMA, and CRA.

#### TEM analysis of nano-SiO<sub>2</sub> extracted from RA (0.5% nano-SiO<sub>2</sub>)

When nano-SiO<sub>2</sub> is homogeneously coated by PA6 matrix, a chemical bonding is formed between functionalized nano-SiO<sub>2</sub> and PA6, thereby enhancing the interfacial interaction and improving the mechanical strength of PA6-matrix composites.<sup>12</sup> Such enhanced interfacial interaction may also help to improve the dispersibility of nano-SiO<sub>2</sub> in PA6 matrix. Figure 4 shows typical TEM pictures of the original nano-SiO<sub>2</sub> (Figure 4a) and nano-SiO<sub>2</sub> extracted from RA containing 0.5% SiO<sub>2</sub> (Figure 4b, mass fraction; the same hereafter). This nanocomposite sample is selected as a typical example, since it has the best mechanical strength among various tested nanocomposite samples with different contents of nano-SiO<sub>2</sub>. As shown in Figure 4, the morphology of nano-SiO<sub>2</sub> extracted from RA is almost the same as that of the original nano-SiO<sub>2</sub>. However, the size of nano-SiO<sub>2</sub> extracted from nanocomposites is obviously larger. Furthermore, nano-SiO<sub>2</sub> particulates extracted from RA with a “string of bead-like” structure and a diameter of about 30 nm are well coated by PA6 molecular chains. This reveals that there is strong interfacial interaction between nano-SiO<sub>2</sub> and PA6 matrix. Besides, the reactive amino group on the surface of nano-SiO<sub>2</sub> allows continual growth of PA6 molecular chains during the preparation process of PA6, which is beneficial to improve the compatibility of nano-SiO<sub>2</sub> with the polymer matrix and to increase its dispersibility as well. Moreover, functionalized “micro-network-like” nano-SiO<sub>2</sub> particulates dispersed in PA6 matrix may also favor to improve the toughness and avoid the stress concentration of the nanocomposites upon impacting.<sup>22,23</sup>

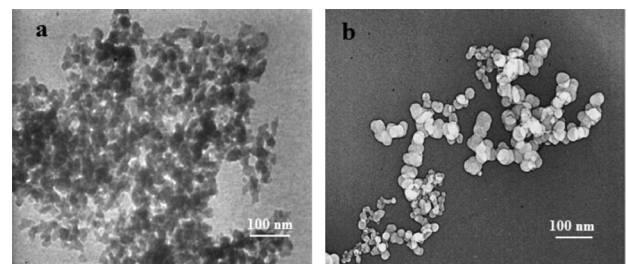


**Figure 4.** TEM photos of the original nano-SiO<sub>2</sub> (a) and nano-SiO<sub>2</sub> extracted from RA

#### SEM analysis of fractured surfaces of PA6 and RA containing 0.5% nano-SiO<sub>2</sub>

Figure 5 shows the SEM images of the fractured surfaces of cast molded PA6 and RA with 0.5% nano-SiO<sub>2</sub>. The fractured surface of PA6 seems to be smooth and shows no obvious signs of plastic flowing (Figure 5a),

corresponding to brittle failure of homogenous materials. Differing from the fractured surface of PA6, the fractured surface of RA shows obvious sign of plastic deformation and contains many micro-cracks and rough fractured pieces (Figure 5b). It corresponds to improved toughness, owing to the existence of modification layer derived from silane coupling agent or prepolymer of PA6 on nano-SiO<sub>2</sub> surface.<sup>14</sup>

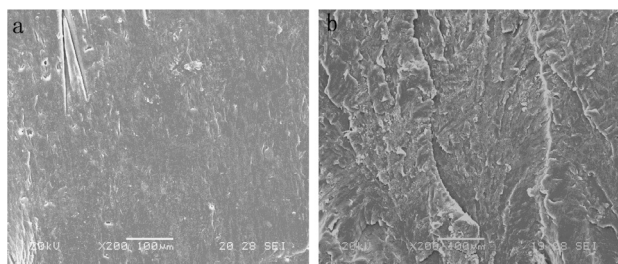


**Figure 5.** SEM micrographs of impact-fractured surfaces of PA6 (a) and RA containing 0.5% nano-SiO<sub>2</sub> (b).

#### XRD and polarizing optical microscopic analyses of PA6 and RA

XRD and polarizing optical microscopy are powerful in analyzing the crystalline structure of PA6. Figure 6 comparatively presents the XRD patterns of PA6 and RA containing 0.5% nano-SiO<sub>2</sub>. The diffraction peaks around 19° and 23° correspond to  $\alpha$  crystalline form, and that at 21° corresponds to  $\gamma$  crystalline form of PA6.<sup>24-26</sup> As seen in Figure 6, RA has weaker  $\alpha$  crystalline form and obviously stronger  $\gamma$  crystalline form than pure PA6. This is possibly because that nano-SiO<sub>2</sub> introduced into the reaction system may act to increase the viscosity of the reaction system. Moreover, it hinders the movement of molecular chains of PA6, while PA6 crystal continually grows. However,

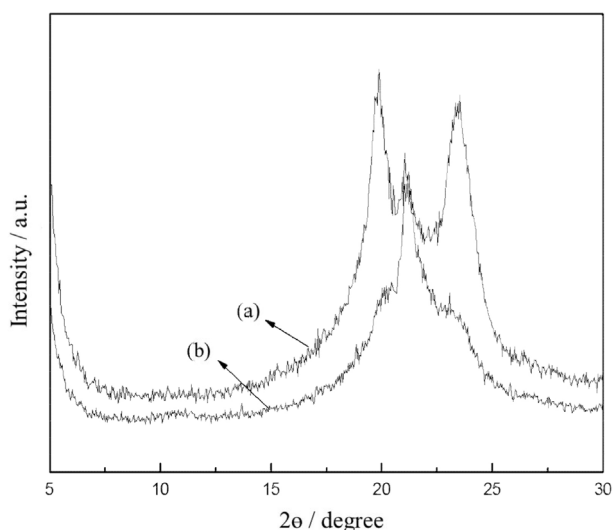


**Figure 6.** XRD patterns of PA6 (a) and RA (b) containing 0.5% nano-SiO<sub>2</sub>.

as-formed strong  $\gamma$  crystalline form is beneficial to increase the impact toughness of PA6, as verified in Figure 9.

Usually, spherocrystal PA6 is more complete and larger than its nanocomposites, and it shows clear black cross extinction in polarization optical microscopic photo.<sup>19,27</sup> Figure 7 shows the polarization optical microscopic photos of PA6 and RA containing 0.5% nano-SiO<sub>2</sub>. It is seen that the size of spherocrystal RA (Figure 7b) is obviously smaller than that of PA6 (Figure 7a), and the completeness of the latter also seems to be poorer. This is mainly because nano-SiO<sub>2</sub> with heterogeneous nucleation effect hinders the growth and reduces the completeness of PA6 spherocrystal.<sup>23</sup>

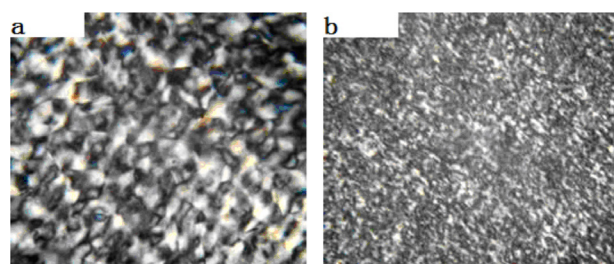


**Figure 7.** Polarizing optical microscopic photos of PA6 (a) and RA containing 0.5% nano-SiO<sub>2</sub> (b).

#### DSC analyses of PA6 and RA

Figure 8 shows the DSC curves of PA6 and RA with 0.5% nano-SiO<sub>2</sub>. Corresponding characteristic crystal parameters are presented in Table 1. As seen in Figure 8a, nano-SiO<sub>2</sub> has almost no effect on the melting temperature of PA6 matrix. However, the crystallization temperature of RA gradually decreases with increasing dosage of nano-SiO<sub>2</sub> (Figure 8b), which well conforms to the hindering effect of nano-SiO<sub>2</sub> to the movement of PA6 molecular chains. This can be better illustrated by taking into account the characteristic crystal parameters in Table 1. Namely, the crystallinity ( $\chi_c$ ) of RA is slightly larger than that of PA6, which suggests that nano-SiO<sub>2</sub> particulates possess a strong heterogeneous nucleation capability. However, the full width at half maximum of crystallization peak ( $\Delta T_{c1/2}$ ), i.e., the crystallization rate, of RA is smaller than that of PA6 and it gradually decreases with increasing dosage of SiO<sub>2</sub>, which is because SiO<sub>2</sub> nanoparticles hinder the movement and limit the diffusion process of PA6 chains.<sup>24</sup> A comparison of the heat of melting ( $\Delta H_c$ ) of PA6 and its nanocomposites also confirms that PA6-matrix nanocomposites have reduced crystallization rate than PA6. The reason lies in that, with increasing content of nano-SiO<sub>2</sub>, more silica nanoparticles function to hinder the movement of PA6 molecular chains. Therefore, the crystallization of RA is dependent on a compromise

**Table 1.** Characteristic crystal parameters of PA6 and RA

Sample	$T_m / ^\circ\text{C}$	$\Delta H_m / (\text{J g}^{-1})$	$T_c / ^\circ\text{C}$	$\Delta H_c / (\text{J g}^{-1})$	$\chi_c / \%$	$\Delta T_{c1/2} / \text{min}$
PA6	219.52	54.02	185.48	60.68	26.37	0.42
PA6 with 0.1% nano-SiO <sub>2</sub>	218.02	56.93	185.01	60.84	26.44	0.53
PA6 with 0.3% nano-SiO <sub>2</sub>	217.58	57.72	183.92	61.85	26.88	0.51
PA6 with 0.5% nano-SiO <sub>2</sub>	217.27	59.73	183.85	62.79	27.29	0.56
PA6 with 0.7% nano-SiO <sub>2</sub>	219.52	56.43	182.23	60.31	26.21	0.59
PA6 with 0.9% nano-SiO <sub>2</sub>	219.01	55.23	182.97	63.14	27.44	0.58

$T_m$ : melting temperature;  $T_c$ : crystallization temperature;  $\Delta H_m$ : heat of melting;  $\Delta H_c$ : heat of crystallization;  $\chi_c$ : crystallinity; and  $\Delta T_{c1/2}$ : full width at half maximum of crystallization peak.

between the heterogeneous nucleation effect and hindering effect of nano-SiO<sub>2</sub>.

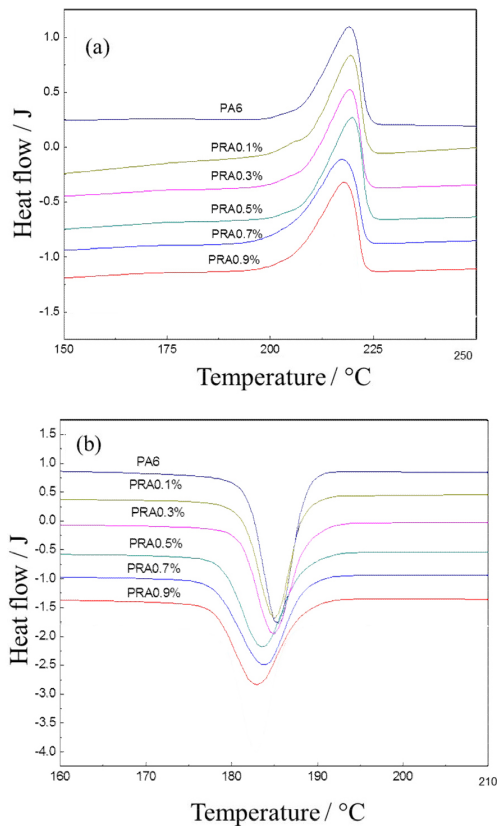


**Figure 8.** Melting behaviors (a) and crystallization behaviors (b) of PA6 and RA.

Mechanical properties of RA and viscosity average molecular weight of PA6 extracted from RA containing different nano-SiO<sub>2</sub> contents

The effect of nano-SiO<sub>2</sub> on the tensile strength and impact strength of as-fabricated RA is shown in Figure 9. It is seen that the mechanical properties gradually increase with increasing content of nano-SiO<sub>2</sub> up to 0.5%. In other words, RA with 0.5% nano-SiO<sub>2</sub> has the

maximum tensile strength and impact strength, which are higher than those of PA6 matrix by 54.4% and 38.7%, respectively. Thus, masterbatch method combined with *in situ* polymerization is obviously super to molten mixing technique and direct *in situ* polymerization route in terms of the ability to improve the mechanical properties of PA6-matrix composites. This should be closely related to the improvement of interfacial adhesion between reactive nano-SiO<sub>2</sub> filler prepared via masterbatch route and PA6 matrix.<sup>12</sup> Namely, owing to the presence of hydrogen bonds and chemical bonding, PA6 molecular chains are easily connected to the surface of nano-SiO<sub>2</sub> to form high-density interfacial zone between PA6 and nano-SiO<sub>2</sub>, which should favor to increase the stiffness of PA6/SiO<sub>2</sub> nanocomposites. Besides, the modification layer derived from silane coupling agent or PA6 prepolymer on nano-SiO<sub>2</sub> surface is beneficial to improving the toughness of the nanocomposites.<sup>14</sup> However, when the dosage of nano-SiO<sub>2</sub> exceeds 0.5%, the dispersion of the nanoparticles in PA6 matrix is worsened, and the adhesion of the nanoparticles by PA6 coated layer is reduced accordingly. The aggregation of nano-SiO<sub>2</sub> forms stress concentration point to hinder

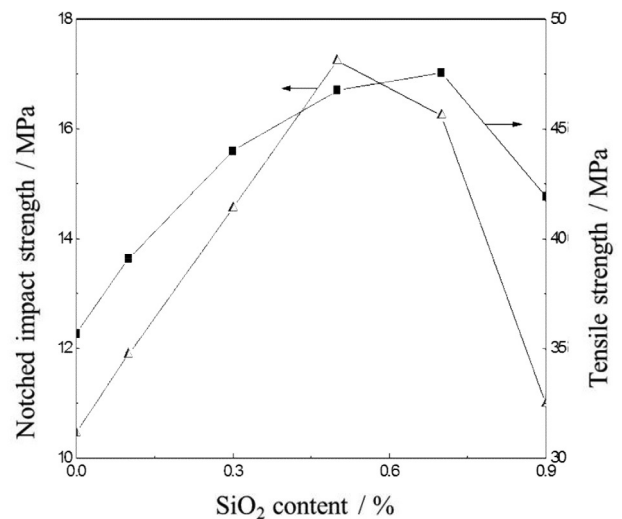


**Figure 9.** Mechanical properties of PA6 and RA.

stress propagation, thereby leading to reduced mechanical properties of polymeric materials.<sup>1,16,19</sup>

Moreover, the molecular weight of PA6 may also vary greatly with increasing dosage of nano-SiO<sub>2</sub>, thereby affecting the mechanical properties. As seen in Figure 10, the viscosity average molecular weight ( $\overline{M}\eta$ ) of PA6/nano-SiO<sub>2</sub> nanocomposites gradually decreases with increasing content of SiO<sub>2</sub>. This is mainly because, when Ubbelohde viscometer is performed to determine the viscosity ( $\eta$ ) of PA6/nano-SiO<sub>2</sub> composites dissolved in formic acid, as-measured  $\eta$  tends to increase gradually with increasing SiO<sub>2</sub> content, due to reduced motion of PA6 molecular chains. As a result, both the molecular weight and tensile strength of PA6/nano-SiO<sub>2</sub> composites tend to decrease at a too high content of nano-SiO<sub>2</sub>.

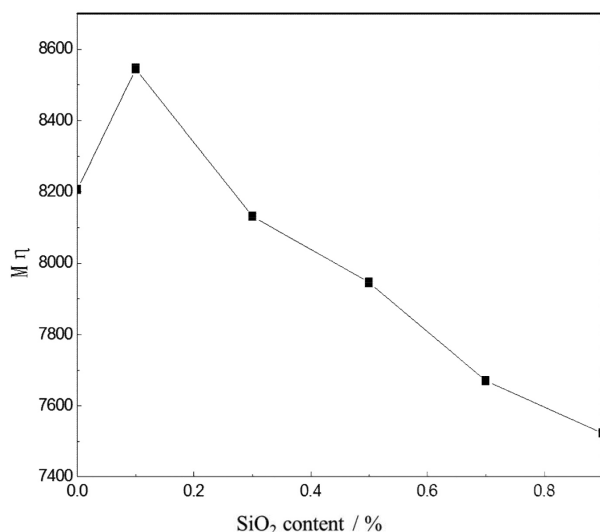


**Figure 10.** Viscosity average molecular weight ( $\overline{M}\eta$ ) of PA6 extracted from RA containing different nano-SiO<sub>2</sub> contents.

## Conclusions

A reactive polymerized  $\epsilon$ -caprolactam masterbatch containing a high content of nano-SiO<sub>2</sub> was prepared by *in situ* polymerization of  $\epsilon$ -caprolactam. The nano-SiO<sub>2</sub> particles contained the amino group that originated from the silane coupling agent 3-triethoxysilylpropylamine. The amino groups on nano-SiO<sub>2</sub> surface can react with the monomer and prepolymers to form a flexible interface. The as-obtained reactive masterbatch employed as a filler is able to continually participate in the ring-opening polymerization process of  $\epsilon$ -caprolactam, thereby affording PA6 composites possessing improved mechanical properties. In other words, PA6 molecular chains are anchored on nano-SiO<sub>2</sub> surface through chemical bonding, thereby increasing the compatibility of nano-SiO<sub>2</sub> with the PA6 matrix and improving its dispersibility as well.

Besides, the crystallization behavior of RA is dependent on a compromise between the heterogeneous nucleation effect and hindering effect of nano-SiO<sub>2</sub>. In one word, the masterbatch method combined with *in situ* polymerization is superior to the conventional molten mixing technique and the direct *in situ* polymerization route for the fabrication of PA6-matrix composites with improved mechanical properties.

## Acknowledgments

This research is financially supported by the Ministry of Science and Technology of China (project of '973' plan; grant No. 2013CB63303), Henan Provincial Natural Science Foundation of China (grant No. 1121012104000), and National Natural Science Foundation of China (grant No. 21371050).

## References

- Hasan, M. M.; Zhou, Y. X.; Mahfuz, H.; Jeelani, S.; *Mater. Sci. Eng., A* **2006**, *429*, 181.
- Mahfuz, H.; Hasan, M.; Dhanak, V.; Beamson, G.; Stewart, J.; Rangari, V.; Wei, X.; Khabashesku, V.; Jeelani, S.; *Nanotechnology* **2008**, *19*, 1.
- Duan, J. K.; Shao, S. X.; Li, Y.; Wang, L. F.; Jiang, P. K.; Liu, B. P.; *Iran. Polym. J.* **2012**, *21*, 109.
- Morshed, A. K. M. M.; Paul, T. C.; Khan, J.; *Appl. Therm. Eng.* **2013**, *51*, 1135.
- Senthilkumar, V.; Balaji, A.; Narayanasamy, R.; *Mater. Des.* **2012**, *37*, 102.
- Lepoittevin, B.; Pantoustier, N.; Devalckenaere, M.; Alexandre, M.; Calberg, C.; Jérôme, R.; *Polymer* **2003**, *44*, 2033.
- Gu, H.; Tadakamalla, S.; Zhang, X.; Huang, Y. D.; Jiang, Y.; Colorado, H. A.; *J. Mater. Chem. C* **2013**, *1*, 729.
- Yoo, Y.; Spencer, M. W.; Paul, D. R.; *Polymer* **2011**, *52*, 180.
- Shi, Y.; Peterson, S.; Sogah, D. Y.; *Chem. Mater.* **2007**, *19*, 1552.
- Schmidt, D.; Shah, D.; Giannelis, E. P.; *Curr. Opin. Solid State Mater. Sci.* **2002**, *6*, 205.
- Rudzinski, S.; Häussler, L.; Harnisch, Ch.; Mäder, E.; Heinrich, G.; *Compos. Part A-Appl. S.* **2011**, *42*, 157.
- Xu, X. M.; Li, B. J.; Lu, H. M.; Zhang, Z. J.; Wang, H. G.; *Appl. Surf. Sci.* **2007**, *254*, 1456.
- Shah, R. K.; Paul, D. R.; *Polymer* **2004**, *45*, 2991.
- Benali, S.; Peeterbroeck, S.; Brocorens, P.; Monteverde, F.; Bonnaud, L.; Alexandre, M.; *Eur. Polym. J.* **2008**, *44*, 1673.
- McLauchlin, A.; Bao, X. J.; Zhao, F.; *Appl. Clay Sci.* **2011**, *53*, 749.
- Li, Y.; Yu, J.; Guo, Z. X.; *J. Appl. Polym. Sci.* **2002**, *84*, 827.
- Coleman, M. M.; Skrovanek, D. J.; Hu, J. B.; Paul, C. P.; *Macromolecules* **1988**, *21*, 59.

18. Coleman, M. M.; Lee, K. H.; Skrovanek, D. J.; *Macromolecules* **1986**, *19*, 699.
19. Shu, H. D.; Liu, K.; Liu, F.; *J. Appl. Polym. Sci.* **2013**, *129*, 2931.
20. Schaeffgen, J. R.; Trivisonno, C. F.; *J. Am. Chem. Soc.* **1951**, *73*, 4580.
21. Pant, H. R.; Bajgai, M. P.; Yi, C.; *Colloid. Surf. A* **2010**, *370*, 87.
22. Wang, Z. C.; Suo, J. P.; Li, J.; *J. Appl. Polym. Sci.* **2009**, *114*, 2388.
23. Xu, X. M.; Li, B. J.; Lu, H. M.; Zhang, Z. J.; Wang, H. G.; *J. Appl. Polym. Sci.* **2008**, *107*, 2007.
24. Ho, J. Ch.; Wei, K. H.; *Macromolecules* **2000**, *33*, 5181.
25. Fornes, T. D.; Paul, D. R.; *Polymer* **2003**, *44*, 3945.
26. Zhao, Z. D.; Zheng, W. T.; Tian, H. W.; Yu, W. X.; Han, D.; Li, B.; *Mater. Lett.* **2007**, *61*, 925.
27. Fu, P.; Wang, M. L.; Liu, M. Y.; Jing, Q. Q.; Cai, Y.; Wang, Y. D.; Zhao, Q. X.; *J. Polym. Res.* **2011**, *18*, 651.

Submitted on: January 22, 2014

Published online: May 13, 2014